The Membrane-Dipped Neuronal SNARE Complex: A Site-Directed Spin Labeling Electron Paramagnetic Resonance Study†

Dae-Hyuk Kweon, Chang Sup Kim, and Yeon-Kyun Shin*

Department of Biochemistry, Biophysics, and Molecular Biology, Iowa State University, Ames, Iowa 50011

Received April 8, 2002; Revised Manuscript Received May 16, 2002

ABSTRACT: The formation of the soluble *N*-ethylmaleimide-sensitive factor attachment protein receptor (SNARE) complex is an essential process for membrane fusion and the neurotransmitter release in neurons. As an initial step toward the determination of the membrane topology of the SNARE complex, residues at the membrane−water interface were investigated with site-specific spin labeling electron paramagnetic resonance. EPR analysis revealed that the basic amino acid-rich interfacial region, which is universal for all transmembrane SNARE proteins, inserts into the membrane, eliminating the gap between the core complex and the membrane. The result raises the possibility that core complex formation directly leads to the apposition of two membranes, which could facilitate membrane fusion.

In eukaryotic cells transport vesicles constantly shuttle between compartments, delivering proteins, hormones, or neurotranmitters to the designated destinations. Vesicular transport is fundamental to the maintenance of physical and functional identities of organelles and proper cell growth, as well as to communication among neurons. It is remarkable that all transport by vesicles uses the same or similar protein machinery that facilitates fusion of vesicles to the target membrane. Soluble *N*-ethylmaleimide-sensitive factor attachment protein receptor (SNARE)[1] proteins are essential components of this highly conserved fusion machinery (*1*−*4*). Assembly of vesicle-associated (v-) SNAREs with the target membrane (t-) SNAREs is required for membrane fusion.

The SNARE family involved in neurotransmission is one of the best characterized systems biochemically and biophysically. t-SNARE proteins syntaxin 1A and SNAP-25 reside on the plasma membrane to which syntaxin 1A is anchored with a single membrane-spanning α-helix. Upon docking of the delivery vesicle to the plasma membrane the vesicle-associated membrane protein 2 (VAMP2) interacts with t-SNAREs to form a stable complex (*5*−*7*). The key feature of SNARE assembly is the formation of a parallel four-helix bundle in the soluble part (*8*, *9*) that could help to bring about membrane fusion. However, it is unknown how the soluble domains are adjoined to membranes, and consequently, it is not understood the way core complex formation drives two membranes into fusion.

As a first step toward the determination of the structure and membrane topology of the SNARE complex using site-directed spin labeling EPR (*10*, *11*), 12 consecutive residues at the membrane−water interface were substituted to cysteines and modified with a nitroxide spin label. EPR saturation analysis revealed that the basic amino acid-rich interfacial region, which is universal for all transmembrane SNARE proteins, inserts into the membrane, implying the direct coupling of the SNARE core to the membrane. The EPR data suggest the possibility that core complex formation directly leads to the merging of two membranes.

EXPERIMENTAL PROCEDURES

Protein Expression and Purification. Full-length syntaxin 1A (aa 4−288), the soluble domain of VAMP2 (aa 1−94), and the C-terminal SNARE motif of SNAP-25 (SNAP-25-[C]) (aa 125−206) were expressed in *Escherichia coli* as glutathione *S*-transferase (GST) fusion protein and were purified using glutathione−agarose chromatography. SNARE proteins were cleaved off from the GST-bound resin part by thrombin. The N-terminal SNARE motif of SNAP-25 (SNAP-25[N]) (aa 1−82) was expressed as a His_6-tagged protein and was purified using Ni-NTA resin (Qiagen).

Site-Directed Spin Labeling. For syntaxin 1A three native cysteine residues, C145, C271, and C272, were changed to alanines in order to introduce a unique cysteine site specifically for the nitroxide attachment. Cysteine mutants were generated by the QuickChange site-directed mutagenesis kit (Stratagene), and they were confirmed by DNA sequencing. Cysteine mutants of syntaxin 1A were reacted with (1-oxy-2,2,5,5-tetramethylpyrrolinyl-3-methyl)methanethiosulfonate (MTSSL) while the protein is bound to the resin.

Preparation of the SNARE Complex. While the His_6-tagged SNAP-25[N] was bound to Ni−agarose resin, an approximately 2-fold (5-fold for VAMP2) excess of other purified SNARE components was added to form the SNARE

† Support for this work is provided by National Institutes of Health Grant GM51290.

* Corresponding author. E-mail: colishin@iastate.edu. Phone: (515) 294-2530. Fax: (515) 294-0453.

[1] Abbreviations: EPR, electron paramagnetic resonance; GST, glutathione *S*-transferase; IPTG, isopropyl β-D-galactopyranoside; MTSSL, (1-oxy-2,2,5,5-tetramethylpyrrolinyl-3-methyl)methanethiosulfonate spin label; OD_{600}, optical density at 600 nm; PBST-Met, phosphate-buffered saline, pH 7.4, 0.05% (v/v) Tween-20, and 10 mM L-methionine; SNAP-25, synaptosome-associated protein of 25 kDa; SNARE, soluble *N*-ethylmaleimide-sensitive factor attachment protein receptor; VAMP2 (or v-SNARE), vesicle-associated membrane protein 2.

10.1021/bi025934+ CCC: $22.00
Published on Web 06/27/2002

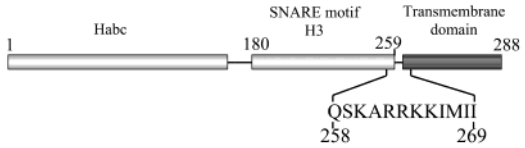

FIGURE 1: Structural elements of full-length syntaxin 1A. Habc is the α-helical domain that dissociates from the H3 domain upon SNARE complex assembly. The H3 domain of syntaxin 1A is the SNARE motif that participates in mediating the SNARE complex assembly. The site-directed spin labeling EPR experiment was carried out in the region of amino acids 258−269 that connects the H3 domain and the transmembrane domain (TMD). The amino acid sequence of this region is displayed.

complex. The mixture was incubated at 4 °C for 24 h. After extensive washing to remove the unbound proteins, the ternary complex was eluted with a buffer containing 250 mM imidazole and 1% *n*-octyl glucoside (OG). The formation of the ternary complex was confirmed with SDS−PAGE.

Membrane Reconstitution. Large unilamellar vesicles (LUV) of 100 nm diameter were prepared using an extruder as described elsewhere. Vesicles of 1-palmitoyl-2-oleoylphosphatidylcholine containing 20 mol % 1-palmitoyl-2-oleoylphosphatidylglycerol were first disturbed by *n*-octyl glucoside (1%) before the detergent-dissolved SNARE complex was added. After incubation for 2 h at room temperature the detergent was removed by treating the solution with Bio-Beads SM2 (Bio-Rad). The final protein concentration was in the range of 30−50 μM.

EPR and Accessibility Measurements. EPR measurements were performed with a Bruker 300E ESP spectrometer equipped with a loop-gap resonator. The gas exchange to the protein sample was achieved with the TPX EPR tube for the loop-gap resonator. For individual mutants power saturation curves were obtained from the peak-to-peak amplitude of the central line ($M = 0$) of the first-derivative EPR spectrum as a function of incident microwave power in the range 0.1−40 mW. Three power saturation curves were obtained after equilibration: (1) with N_2, (2) with air (O_2), and (3) with N_2 in the presence of 200 mM Ni-EDDA (nickel ethylenediaminediacetic acid). From saturation curves, the microwave power $P_{1/2}$ where the first-derivative amplitude is reduced to one-half of its unsaturated value was calculated. The quantity $\Delta P_{1/2}$ is the difference in $P_{1/2}$ values in the presence and absence of a paramagnetic reagent. The $\Delta P_{1/2}$ value is proportional to the collision frequency of the nitroxide to the freely diffusing reagents such as oxygen and Ni-EDDA. Thus, $\Delta P_{1/2}$ is considered to be equivalent to the accessibility W. The immersion depth is calculated on the basis of the reference curves determined from a set of lipid molecules spin labeled at different acyl chain positions.

RESULTS

Site-Directed Spin Labeling EPR. To investigate the membrane topology of the SNARE complex using site-directed spin labeling EPR, residues of full-length syntaxin 1A near the membrane−water interface were replaced with cysteines to which a nitroxide spin label was attached. We prepared 12 cysteine mutants (Q258C−I269C) to explore the interfacial region with the nitroxide spin label (Figure 1). For EPR measurements the recombinant complex was assembled from spin-labeled syntaxin 1A, soluble VAMP2,

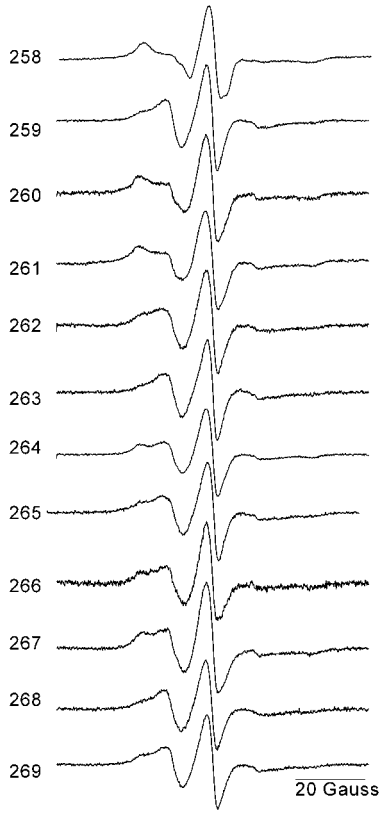

FIGURE 2: First-derivative EPR spectra of spin-labeled SNARE complexes in the membrane taken at room temperature. The recombinant ternary SNARE complex is composed of spin-labeled full-length syntaxin 1A, the soluble domain of VAMP2, and two SNARE motifs from SNAP-25.

and two separate "SNARE motifs" from SNAP-25. The transmembrane domain (TMD) of VAMP2 was not included this time to avoid the interaction between two TMDs in one membrane and to best mimic the trans SNARE complex. All spin-labeled recombinant complexes were capable of forming the sodium dodecyl sulfate- (SDS-) resistant complex, which is one characteristic feature of the complex, as confirmed with SDS−PAGE (data not shown). The SNARE complex was reconstituted into phospholipid vesicles containing 20% negatively charged lipids.

The EPR spectrum is a sensitive function of the motional rate. The slower the motion of the nitroxide side chain, the broader its EPR spectrum (*12*, *13*). EPR spectra taken at room temperature are moderately broad for all SNARE complex samples (Figure 2). The relatively slow motion could have resulted from some tertiary interaction of the nitroxide side chain with other parts of the protein. Alternatively, motion could have been retarded by the insertion of the nitroxide side chains into the viscous membrane environment.

EPR Accessibility Measurements. The EPR accessibility measurement (*14*) has proven to be a powerful technique to probe the insertion of a polypeptide into the membrane (*15*−*17*). For SNARE complex samples accessibility of the nitroxide to a water-soluble paramagnetic reagent Ni-EDDA ($W_{Ni-EDDA}$) was much lower than typical values for fully solvent-exposed nitroxides (Figure 3a). For an exposed nitroxide we anticipate $W_{Ni-EDDA}$ values to be as high as 40 under the same conditions (*18*). This suggests that the nitroxides attached to the SNARE complex are not exposed to the water phase. Again, the polypeptide chain could be

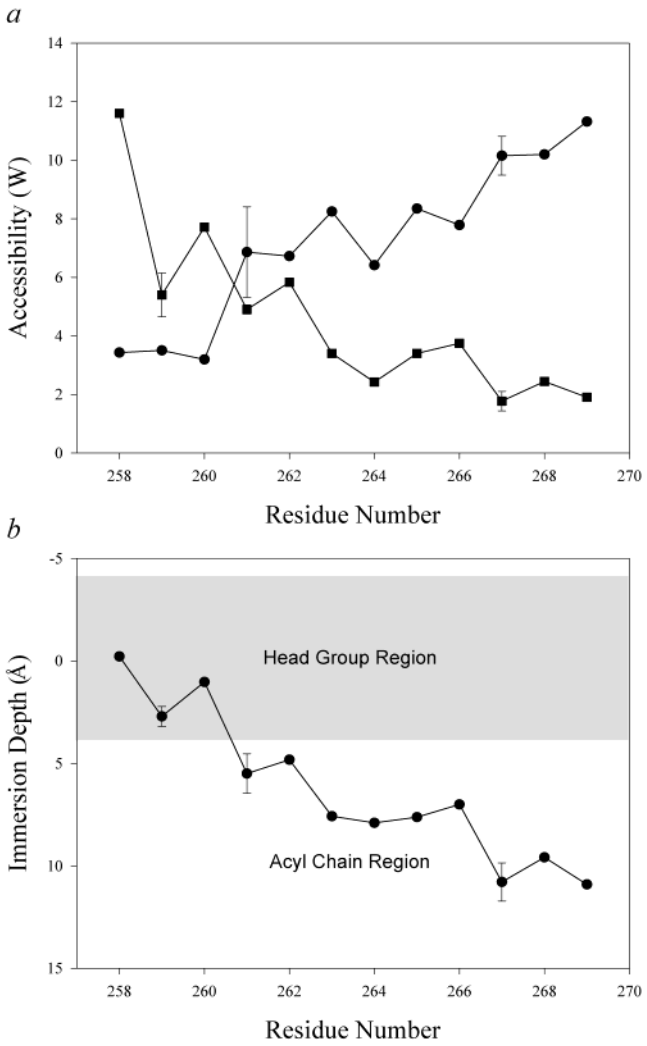

FIGURE 3: Accessibility to the paramagnetic reagents and membrane immersion depths. (a) The accessibility parameter to oxygen (W_{O_2}) (filled circles) and that to Ni-EDDA ($W_{Ni-EDDA}$) (filled squares) was plotted with respect to the residue numbers. (b) Membrane immersion depths for the nitroxides. In the graph the location of the lipid phosphate groups is considered as the 0 depth. The phosphate group is located right in the middle of the headgroup region whose thickness is approximately 8 Å. Only one leaflet of the bilayer is shown.

either inserted into the membrane or buried in the protein environment, consistent with what is inferred from broad EPR spectra.

The distinction between the membrane insertion and the burial in the protein environment can be made by the accessibility parameter to nonpolar oxygen (W_{O_2}). Oxygen heavily prefers the membrane phase to the protein interior. A high W_{O_2} value is a characteristic feature of the membrane-inserted nitroxide. In contrast, the values for the buried nitroxide in the protein environment are often quite low. For SNARE complex samples W_{O_2} values are relatively high for all positions in the range of 7−12 except for somewhat lower values for 258−260 (Figure 3a). These values are similar to the W_{O_2} value of 10 for the phospholipid with the nitroxide at the fifth carbon position of the acyl chain (*19*). Therefore, nitroxides attached at positions 261 through 269 are likely to be inserted into the membrane.

Membrane Immersion Depths of the Basic Interfacial Region. The ratio of $W_{Ni-EDDA}$ to W_{O_2} has been shown to hold a quantitative relationship to the membrane immersion depth (*14*). On the basis of the calibration curve from standard samples of known immersion depths that include the spin-labeled lipids and bacteriorhodopsin, we calculated the immersion depth for the SNARE samples. It appears that the nitroxides at positions 258−260 are located in the headgroup region of the bilayer (Figure 3b). Very interestingly, the EPR data show that the nitroxides at positions 261 through 269 are inserted into the acyl chain region of the membrane.

It was previously thought that the TMD of syntaxin 1A starts from residue 266 that begins the 22 amino acids stretch of the nonpolar residues (*20*). However, the EPR data show that five residues preceding I266 are also inserted into the membrane. Residue 260, which is the last residue of the core helical bundle (*8*), is located near the phosphate group. Thus, it is likely that the C-terminal end of the core coiled coil may be stuck to the headgroup region. Therefore, we conclude that there is no flexible tether between the SNARE core and the membrane.

DISCUSSION

The EPR results are quite intriguing because the amino acid sequence of the interface region (261−265) is ARRKK that appears to be highly hydrophilic with four positive charges. The immersion depth of nitroxides attached to those positions ranges from 5 to 8 Å from the phosphate group of the lipid in the bilayer. Thus, this peptide segment is bound laterally to the membrane and is likely to be unstructured. Consistently, this segment was able to partially tolerate some helix-destabilizing mutations and amino acid insertions into the region (*21*, *22*). However, insertion of as many as 10 additional amino acids was found to be lethal to the function of the protein (*22*). Such a long extra amino acid length in the region would definitely change the topology of the SNARE complex with respect to the membrane. Perhaps the membrane no longer holds its firm grip onto the SNARE core.

Since EPR measures the position of the paramagnetic center of the nitroxide, the immersion depths do not necessarily report the actual location of the peptide backbone. It is possible that the peptide backbone of the ARRKK region is located somewhat shallower than what is measured with EPR, to fulfill the hydrogen-bonding requirement for the peptide backbone. It is also possible that the hydrophobic nature of the nitroxide contributed to some overestimation of the immersion depths. However, at minimum, the peptide backbone must be positioned below the phosphate group, considering that the arm length of the nitroxide side chain is not longer than 7 Å (*23*, *24*). It is highly unlikely that the insertion of the RRKK region is driven by the alteration of the charged residue to the nitroxide. Consistent with this assertion, we observed that the nitroxide attached to A261C, which precedes RRKK, is already immersed 6 Å deep from the phosphate group.

The ionic interaction must have helped the adhesion of the ARRKK region to the membrane (*25*). While the peptide backbone is embedded below the phosphate group, the positive charges on lysines and arginines can snorkel out to seek the negative charges on phosphate. A similar depth and mode of membrane insertion have been found for the positively charged model as well as natural peptides (*26*).

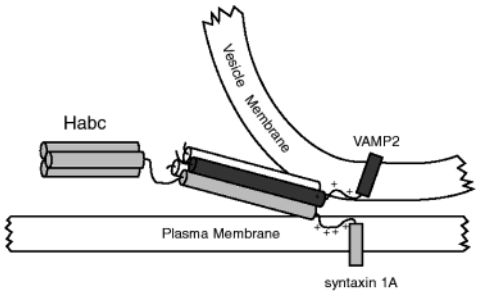

FIGURE 4: Model for SNARE-induced membrane fusion. The highlight of the model is the insertion of the positively charged interfacial regions into membranes. The SNARE core complex tightly pins two membranes to allow the juxtaposition as well as the deformation of membranes. Helices are depicted as cylinders. SNARE proteins are syntaxin 1A (light gray), VAMP2 (dark gray), and SNAP-25 (white). The insertion of the VAMP2 interfacial residues into the membrane is hypothetical and is not experimentally confirmed.

One striking common feature of proteins in the syntaxin family as well as in VAMP family is the cluster of the basic amino acids that separate the core complex and TMD (*20*). Thus, insertion of the basic amino acid-rich region into the membrane may be a universal theme for all proteins in the syntaxin and the VAMP families.

Membrane fusion requires the juxtaposition of two membranes. For viral fusion proteins such as HIV gp41 protein conformational changes supposedly drive two membranes into close proximity (*27*, *28*). Likewise, SNARE assembly to a parallel coiled coil will pull two membranes close to one another. However, there is evidence that "close is not enough" to advance toward membrane fusion (*29*). The merging of two membranes involves the deformation of membranes that requires free energy as much as 25 kcal/mol (*30*). It is widely believed that core complex formation generates the force that could be used for membrane deformation. But the mounting question has been: how does the system harness the available force?

A hypothetical mechanism for membrane fusion has been proposed on the basis of the crystal structure of the SNARE core complex. In this model α-helices of syntaxin 1A and VAMP2 in the core extend all the way through the transmembrane domains with a high degree of bending at the interfacial region (*8*). However, the present EPR results are not consistent with this hypothetical model. We suggest that the direct coupling between the core complex and the plasma membrane is achieved by the lateral insertion of the ARRKK region into the membrane. With the firm grip onto the membrane one can envision that force-producing SNARE assembly directly drags two membranes into contact (Figure 4), leading to the membrane deformation that facilitates membrane fusion.

Although the current EPR data support the new fusion model presented in Figure 4, there are several weaknesses that need to be pointed out and properly addressed with further experimental data. First, the generality of the insertion of the basic interfacial region of SNARE proteins is not established yet. Likewise, the membrane-inserted interfacial domain of VAMP2 in Figure 4 is purely hypothetical. Second, according to the previous studies with basic model peptides the membrane insertion of the RRKK region is likely to provide only a few kilocalories per mole (*31*). It appears that this binding energy may not be enough to sustain the strain in the fusion complex that could be as high as 25 kcal/mol. Perhaps some concerted effort of several SNARE complexes may be necessary to overcome the fusion energy barrier. The multimerization of the SNARE complex (*32*) may be achieved via the interaction of the transmembrane domain (*33*), via the domain swapping (*34*), or via a combination of both.

Although EPR spectra in Figure 2 exhibit mostly intermediate motional rates, we observe composite spectra containing some further immobilized components for positions 260, 261, 264, 266, and 267. It is likely that these immobilized components indicated some tertiary interactions. For positions 260 and 261 nitroxides may have some contact with VAMP2. For the other positions the further immobilized components could be due to the interaction among syntaxin tansmembrane domains (*33*).

REFERENCES

1. Rothman, J. E. (1994) *Nature 372*, 55−63.
2. Jahn, R., and Südhof, T. C. (1999) *Annu. Rev. Biochem. 68*, 863−911.
3. Lin, R. C., and Scheller, R. H. (2000) *Annu. Rev. Cell. Dev. Biol. 16*, 19−49.
4. Brunger, A. T. (2001) *Curr. Opin. Struct. Biol. 11*, 163−173.
5. Bennett, M. K. (1995) *Curr. Opin. Cell Biol. 7*, 581−586.
6. Lin, R. C., and Scheller, R. H. (1997) *Neuron 19*, 1087−1094.
7. Pevsner, J., Hsu, S. C., Braun, J. E., Calakos, N., Ting, A. E., Bennett, M. K., and Scheller, R. H. (1994) *Neuron 13*, 353−361.
8. Sutton, R. B., Fasshauer, D., Jahn, R., and Brunger, A. T. (1998) *Nature 395*, 347−353.
9. Poirier, M. A., Xiao, W., Macosko, J. C., Chan, C., Shin, Y. K., and Bennett, M. K. (1998) *Nat. Struct. Biol. 5*, 765−769.
10. Hubbell, W. L., Gross, A., Langen, R., and Lietzow, M. A. (1998) *Curr. Opin. Struct. Biol. 5*, 649−656.
11. Hubbell, W. L., Cafiso, D. S., and Altenbach, C. (2000) *Nat. Struct. Biol. 9*, 735−739.
12. Mchaourab, H. S., Lietzow, M. A., Hideg, K., and Hubbell, W. L. (1996) *Biochemistry 35*, 7692−7704.
13. Schneider, D. J., and Freed, J. H. (1989) in *Biological Magnetic Resonance* (Berliner, L. J., and Reben, J., Eds.) Vol. 8, pp 1−76, Plenum, New York.
14. Altenbach, C., Greenhalgh, D. A., Khorana, H. G., and Hubbell, W. L. (1994) *Proc. Natl. Acad. Sci. U.S.A. 91*, 1667−1671.
15. Shin, Y. K., Levinthal, C., Levinthal, F., and Hubbell, W. L. (1993) *Science 259*, 960−963.
16. Altenbach, C., Marti, T., Khorana, H. G., and Hubbell, W. L. (1990) *Science 248*, 1088−1092.
17. Barranger-Mathys, M., and Cafiso, D. S. (1996) *Biochemistry 35*, 498−505.
18. Macosko, J. C., Kim, C.-H., and Shin, Y.-K. *J.* (1997) *Mol. Biol. 18*, 1139−1148.
19. Yu, Y. G., Thorgeirsson, T. E., and Shin, Y.-K. (1994) *Biochemistry 33*, 14221−14226.
20. Weimbs, T., Mostov, K., Low, S. H., and Hofmann, K. (1998) *Trends Cell Biol. 8*, 260−262.
21. McNew, J. A., Weber, T., Engelman, D. M., Sollner, T. H., and Rothman, J. E. (1999) *Mol. Cell 4*, 415−421.
22. Wang, Y., Dulubova, I., Rizo, J., and Südhof, T. C. (2001) *J. Biol. Chem. 276*, 28598−28605.
23. Rabenstein, M. D., and Shin, Y. K. (1995) *Proc. Natl. Acad. Sci. U.S.A. 92*, 8239−8243.
24. Langen, R., Oh, K. J., Cascio, D., and Hubbell, W. L. (2000) *Biochemistry 39*, 8396−8405.
25. Montal, M. (1999) *FEBS Lett. 447*, 129−130.
26. Victor, K. G., and Cafiso, D. S. (2001) *Biophys. J. 81*, 2241−2250.
27. Weissenhorn, W., Dessen, A., Harrision, S. C., Skehel, J. J., and Wiley, D. C. (1997) *Nature 387*, 426−430.
28. Chan, D. C., Fass, D., Berger, J. M., and Kim, P. S. (1997) *Cell 89*, 263−273.
29. McNew, J. A., Weber., T., Parlati, F., Johnston, R. J., Melia, T. J., Söllner, T. H., and Rothman, J. E. (2000) *J. Cell Biol. 150*, 105−117.

30. Kuzmin, P. I., Zimmerberg, J., Chizmadzhev, Y. A., and Cohen, F. S. (2001) *Proc. Natl. Acad. Sci. U.S.A. 98*, 7235−7240.
31. Kim, J., Mosior, M., Chung, L. A., Wu, H., and McLaughlin, S. (1991) *Biophys. J. 60*, 135−148.
32. Tokumaru, H., Umayahara, K., Pellegrini, L., Ishizuka, T., Saisu, H., Betz, H., Augustine, G., and Abe, T. (2001) *Cell 104*, 421−432.
33. Margittai M., Otto, H., and Jahn, R. (1999) *FEBS Lett. 446*, 40−44.
34. Kweon, D.-H., Chen, Y., Zhang, F, Poirier, M., Kim, C. S., and Shin, Y.-K. (2002) *Biochemistry 41*, 5449−5452.

BI025934+